PROCEEDINGS, 50th Workshop on Geothermal Reservoir Engineering
Stanford University, Stanford, California, February 10-12, 2025
SGP-TR-229

# Quantifying Geothermal Energy Potential: Numerical Reservoir Modeling of the Massepe Geothermal Field in South Sulawesi, Indonesia

Fikri Rahmansyah, Michael Gravatt, John O'Sullivan and Ken Dekkers

Department of Engineering Science, University of Auckland, 70 Symonds Street, Grafton, Auckland 1010, New Zealand

frah650@aucklanduni.ac.nz; fikri.rahmansyah@gmail.com

**Keywords:** Indonesia, Massepe, geothermal reservoir simulation, uncertainty quantification, AUTOUGH2, Waiwera.

## ABSTRACT

The Massepe Geothermal Field in South Sulawesi, Indonesia, presents sufficient geothermal energy potential as a promising greenfield site. This study focuses on assessing its resource capacity through uncertainty analysis and a natural state model, despite limited direct subsurface exploration. A comprehensive three-dimensional (3D) geological model of the Massepe field was developed using public data and reports, integrating geological, geophysical, geochemical, and spatial datasets with LEAPFROG Energy software. Key formations, fault structures, and the North-South Massepe fault were identified as critical components influencing geothermal fluid flow. Magnetotelluric data helped delineate the alteration zone, while surface manifestation data provided constraints on temperature distribution.

A numerical model compatible with AUTOUGH2 and Waiwera was developed to simulate temperature distribution, fluid flow, and heat transfer processes. The model was calibrated by refining permeability parameters and simulating deep geothermal upflow to replicate the field's natural state. High-performance computing enabled thousands of alternative model simulations, which were conditioned against sparse field data, particularly temperatures beneath the clay cap, primarily located below the Pajalele springs. These simulations underwent Approximate Bayesian Computation (ABC) to generate probabilistic power output estimates. The results confirm a strong geothermal upflow along the North-South Massepe fault, with lateral migration effectively constrained by geological structures. The estimated power output of the field ranges from P90, P50, to P10 values over a 25-year production period.

This study enhances the understanding of geothermal systems in similar non-volcanic geological settings, providing valuable insights for strategic planning and the development of renewable energy resources in Indonesia. The refined resource assessment contributes to optimizing geothermal exploration efforts and supports sustainable energy initiatives in the region.

## 1. INTRODUCTION

Geothermal energy is a key component of Indonesia's renewable energy strategy. Sulawesi, with the third-largest geothermal potential in the country, includes numerous non-volcanic geothermal systems such as the Massepe Geothermal Field. The Massepe Geothermal Field is located in South Sulawesi, approximately 194 km north of Makassar, within the Sidenreng Rappang (Sidrap) Regency (See Figure 1). The geothermal area is situated in a structurally complex region, with the North-South Massepe fault serving as the primary geological control on fluid migration. The region is characterized by moderate topographic relief, with geothermal surface manifestations such as hot springs and altered ground observed in the Pajalele and Alakuang areas.

This study builds upon previous research (Rahmansyah et al., 2024) that developed the geological and numerical reservoir modeling of the Massepe Geothermal Field. The current work shifts the focus towards resource assessment, utilizing uncertainty quantification to refine power output estimates and optimize geothermal resource utilization. A numerical model has been developed to evaluate the geothermal potential of the field, incorporating limited subsurface data with advanced numerical simulation techniques.

Despite limited direct subsurface exploration, uncertainty quantification has been employed to derive probabilistic power output estimates, ensuring a comprehensive understanding of the potential of the field under various geologic and operational scenarios.

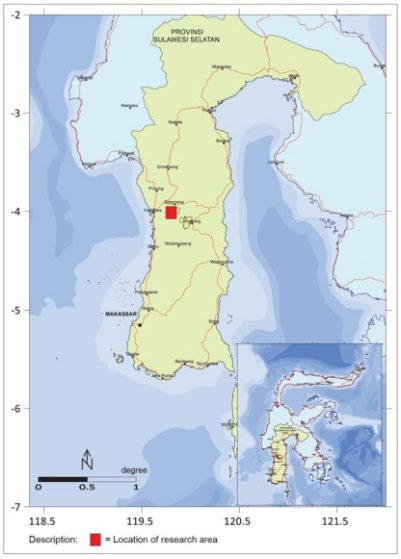


**Figure 1: Map showing the location of the Massepe Geothermal Field (Modified from Joni & Wahyuningsih, 2019, p. 144).**

## 2. CONCEPTUAL MODEL

The conceptual model of the Massepe Geothermal Field was developed by integrating interpretations from geological mapping, resistivity surveys, and geochemical analyses (Rahmansyah et al., 2024). The primary structural control on fluid movement in the system is the North-South Massepe fault, which acts as the main upflow conduit, allowing geothermal fluids to rise from deeper sources. The reservoir is capped by a clay alteration zone, delineated through magnetotelluric (MT) resistivity surveys, which indicates an impermeable barrier that confines the geothermal system and influences fluid flow.

Figure 2 from Rahmansyah et al. (2024) illustrates the map view of the conceptual model, highlighting key fault structures, the location of geothermal manifestations, and the extent of the clay cap. The alignment of these features suggests that hydrothermal fluids ascend along the fault zone and are influenced by the permeability contrast between formations.

Surface geochemical analyses reveal that the Massepe geothermal system is characterized by bicarbonate-sulfate water types, indicative of mixing between geothermal fluids and meteoric water. The Na-K-Mg ternary diagram classifies these waters as immature, implying incomplete chemical equilibrium and a relatively shallow circulation system. Figure 3 from Rahmansyah et al. (2024) presents a cross-section of the conceptual model, showing the geothermal upflow beneath Pajalele and Alakuang hot springs. These manifestations correlate with geophysical anomalies, reinforcing the hypothesis of an active hydrothermal system.

Further characterization of subsurface conditions is required to refine the conceptual model and better constrain reservoir properties. Additional geophysical surveys, such as seismic survey, and exploratory drilling would improve the understanding of permeability variations and reservoir connectivity, which are critical for sustainable geothermal resource development.

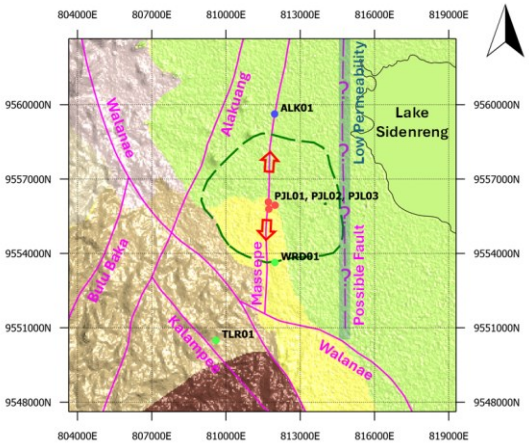


**Figure 2: A top-down view of the conceptual model of the Massepe Geothermal Field, displaying faults (magenta line), bicarbonate-sulfate springs (red dots), bicarbonate springs (green dots), an alkali chloride spring (blue dots), and the clay cap boundary (green dashed line) (Rahmansyah et al., 2024).**

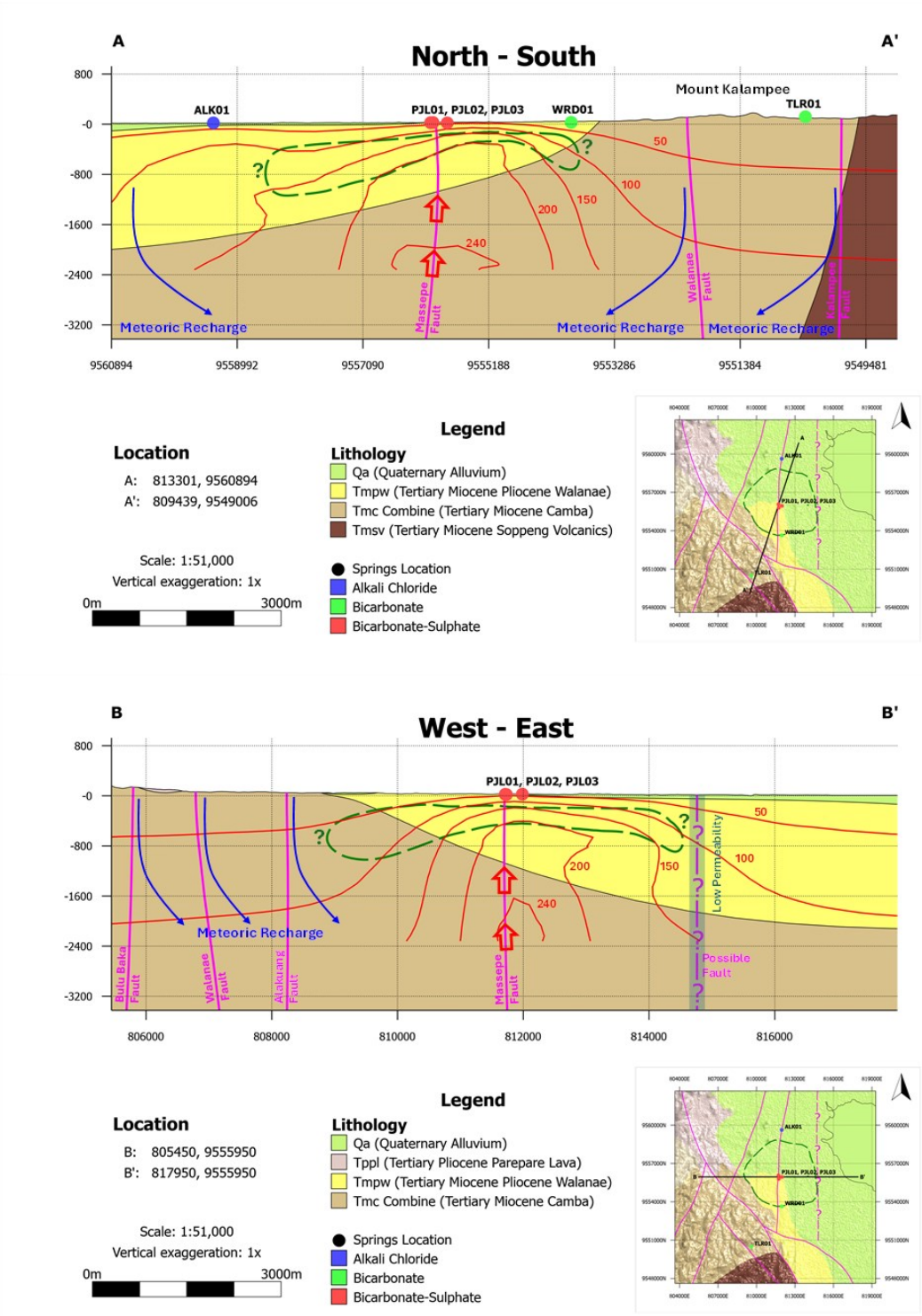


**Figure 3: Cross-sectional views of the conceptual model of the Massepe Geothermal Field, highlighting the clay cap boundary (green dashed line) and the isotherm lines (red line) (Rahmansyah et al., 2024).**

## 3. NUMERICAL RESERVOIR MODEL

A numerical reservoir model is essential for analyzing the natural state of a geothermal system and predicting its response to production and development. The numerical reservoir model of the Massepe field was developed in AUTOUGH2 and Waiwera using a structured grid derived from Leapfrog Energy. This model represents complex permeability structures, incorporating geological formations with enhanced permeability along faults to facilitate fluid movement and heat transfer, ensuring a realistic simulation of reservoir behavior.

To ensure computational efficiency while maintaining accuracy, the grid configuration was refined with vertical and lateral adjustments. Covering an area of 16 km by 15.2 km, the model consists of 34,850 blocks, with refined cells near the North-South Massepe fault, a primary conduit for geothermal upflow (See Figure 4). Grid cell sizes vary from 800 m by 800 m in less dynamic zones to 200 m by 200 m in areas of significant fluid interaction (Rahmansyah et al., 2024).

Boundary conditions were defined to represent natural geothermal processes. The EOS3 module was employed to define the thermophysical properties of water and air, essential for solving mass and energy balance equations (Pruess et al., 1999). The upper boundary simulates atmospheric interactions at 1 bar and 26.5°C, while the lower boundary incorporates a magmatic heat source with a background heat flux of 80 mW/m². Side boundaries were treated as no-flow conditions to confine the modeled geothermal system. Additionally, annual rainfall in the Massepe area, estimated at 1800 mm with a 10% infiltration rate, was incorporated to simulate meteoric recharge, affecting groundwater dynamics and reservoir hydrology (Rahmansyah et al., 2024).

Rock properties were assigned based on lithological classifications, resulting in 79 distinct rock types (Rahmansyah et al., 2024). These variations account for differences in permeability, porosity, and thermal conductivity among lithologies, fault zones, and alteration regions. The assignment of these properties was automated using PyTOUGH to ensure consistency with the geological model (Popineau et al., 2018).

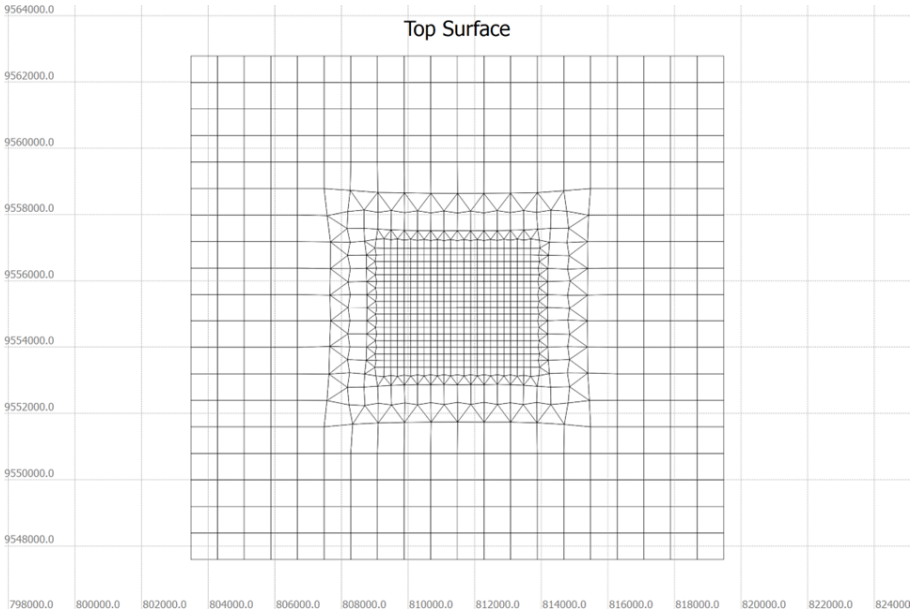


**Figure 4: The map view of the grid arrangement for the Massepe Geothermal Field.**

## 4. NATURAL STATE MODEL

The natural state simulation was conducted to calibrate model parameters, ensuring alignment with observed surface manifestations and estimated subsurface temperatures. The calibration process involved adjusting permeability distributions to match temperature profiles beneath the clay cap, providing a more accurate representation of subsurface conditions.

Figure 5 from Rahmansyah et al. (2024) illustrates the temperature distribution in the natural state model at a depth of 990 meters below sea level. The temperature distribution indicates a well-defined upflow region centered along the North-South Massepe fault, confirming its role as the primary conduit for geothermal fluid migration. Lateral temperature variations highlight the influence of geological structures on fluid flow and heat transfer.

The model calibration process accounted for the absence of available downhole temperature data and the inherent uncertainties in subsurface temperature estimations from geothermometers. Instead, the simulation was refined to closely replicate the argillic alteration in the clay cap, achieving temperatures of approximately 190°C beneath the cap, particularly around the clay dome.

Figure 6 from Rahmansyah et al. (2024) presents a cross-section of mass flow characteristics within the natural state model. The visualization demonstrates the vertical movement of geothermal fluids through permeable fault structures and their lateral migration

within the reservoir. This flow pattern validates the conceptual model, where upflow is concentrated along the Massepe fault, while lateral movement is constrained by adjacent low-permeability formations and an inferred fault to the east of the field.

These results provide confidence in the ability of the model to simulate the natural geothermal system and serve as a foundation for future resource assessment and production simulations.

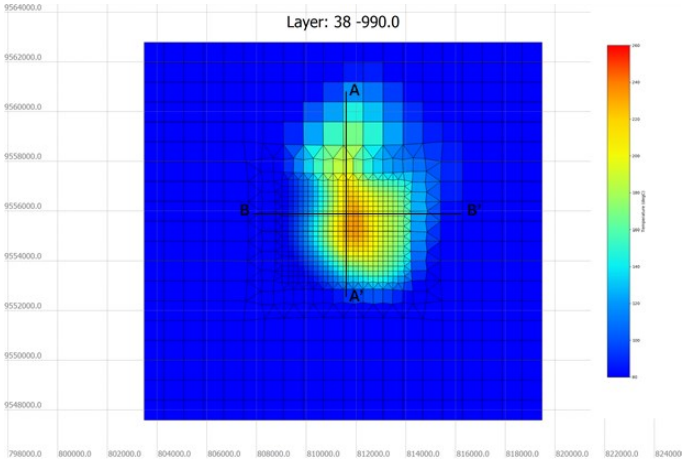


**Figure 5: The temperature distribution in the natural state model at layer 38, located 990 meters below sea level (Rahmansyah et al., 2024).**

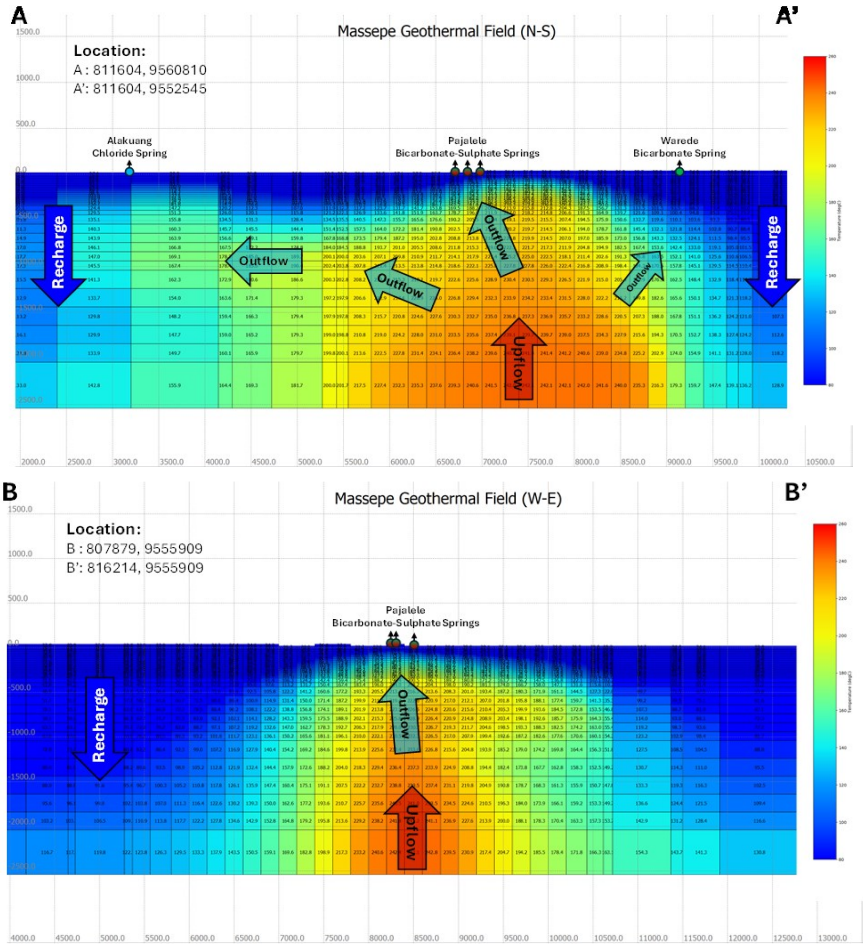


**Figure 6: Temperature distribution and mass flow behavior in the natural state model of the Massepe Geothermal Field. (Top: North-South path along the Massepe fault, Bottom: West-East path crossing Pajalele hot springs) (Rahmansyah et al., 2024)**

## 5. RESOURCE ASSESSMENT

Assessing geothermal energy potential is crucial for determining viable thermal energy for power generation or direct use. Conventional resource estimation relies on stored heat calculations using parameters like temperature, rock density, specific heat, porosity, and volume, though these often involve uncertainties (Dekkers et al., 2022).

This study enhances resource assessment by integrating numerical reservoir modeling with uncertainty quantification. By incorporating reservoir and wellbore physics alongside realistic energy extraction scenarios (Dekkers et al., 2022), this approach refines estimates using natural state modeling. Key factors such as rock properties, fault formations, and upflow characteristics are varied systematically, generating multiple models. The most geologically reasonable models are selected through random sampling for future scenario simulations, ensuring a robust probabilistic evaluation of geothermal potential.

### 5.1 Parameter Samples

To ensure a robust representation of the geothermal reservoir, parameter sampling was conducted by generating 1,000 model realizations with variations in key reservoir properties. The sampled parameters included permeability distributions, reservoir porosity, upflow mass flow, and upflow enthalpy. These variations aimed to capture the range of geological uncertainties that could influence reservoir performance. The sampling process was based on a probabilistic approach, ensuring that each realization represented a reasonable geological scenario.

Figure 7 presents the total mass upflow and heat upflow distributions for the Massepe model, illustrating the variability in mass and heat input across different model realizations. The spread in values highlights the influence of uncertainty in upflow characteristics, which significantly impact the reservoir's thermal structure and energy extraction potential. Additionally, Figure 8 demonstrates the spatial distribution of total upflow at a representative depth layer, showing areas of high and low upflow within the reservoir.

Figure 9 illustrates the permeability distribution within the Walanae sedimentary rock and the Massepe fault, showing how fault rock permeability is modified in different directions. The k1 permeability, aligned West-East, exhibits a reduction across the fault, indicating a permeability barrier. Meanwhile, k2 (North-South) and k3 (vertical) permeability values are enhanced, suggesting preferential fluid flow pathways along and through the fault structure. These permeability variations significantly influence the reservoir's fluid dynamics and overall geothermal potential. The incorporation of these sampled parameters into the model ensures that the assessment captures the full range of possible reservoir behaviors, thereby improving the reliability of subsequent uncertainty quantification and production scenario analyses.

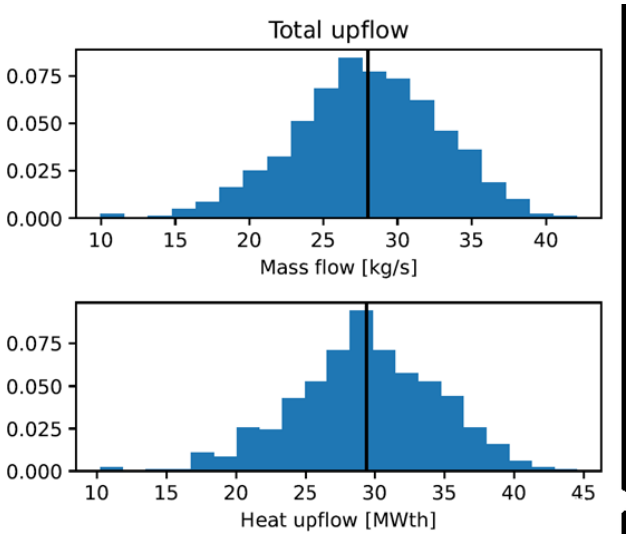


**Figure 7: The distribution of total mass upflow and heat upflow for the Massepe model.**

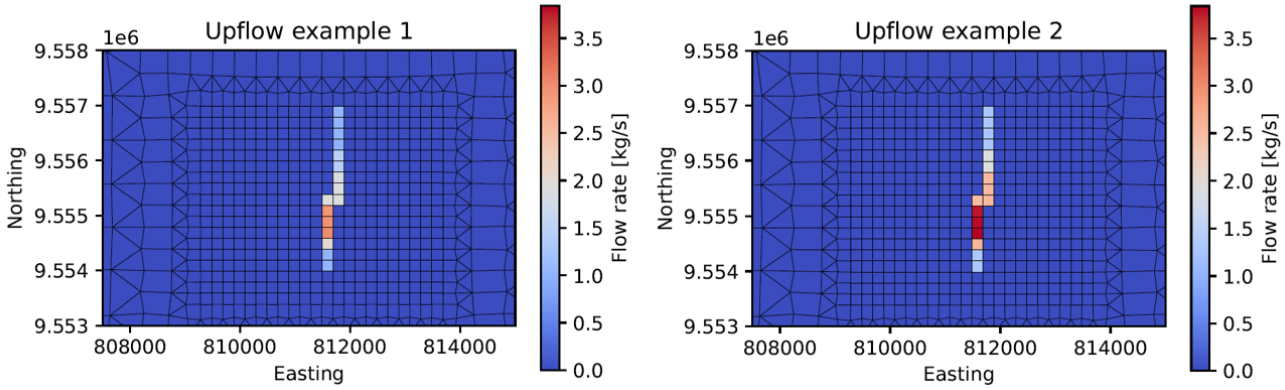


**Figure 8: Examples of the total upflow distribution at layer 44 along the Massepe fault.**

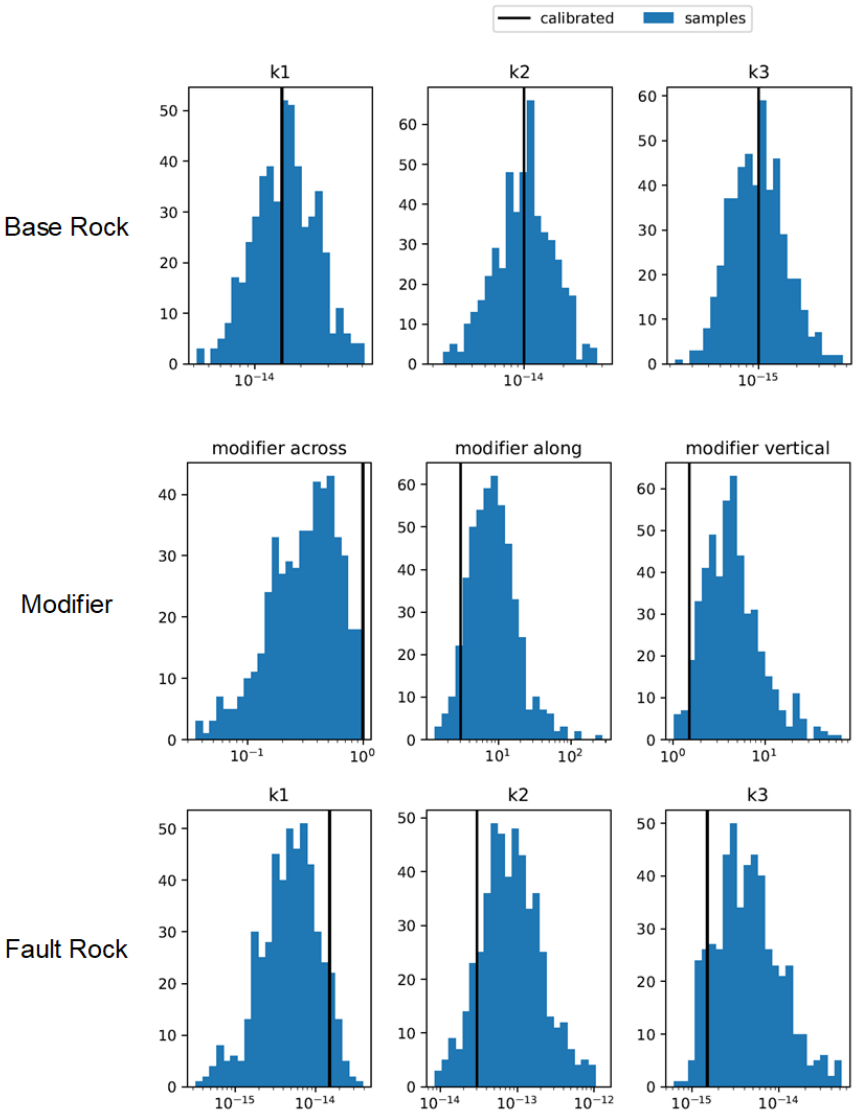


**Figure 9: The permeability distribution of the Walanae sedimentary rock within the reservoir (Top) is adjusted by the modifier (Middle), leading to the Massepe fault (Bottom).**

### 5.2 Conditioned Samples

A total of 1,000 model realizations were generated with variations in permeability, upflow mass flow, upflow enthalpy, and reservoir porosity to account for geological uncertainties. These realizations were evaluated using Approximate Bayesian Computation (ABC) to ensure consistency with observed temperatures beneath the clay cap. The ABC method, implemented via the ccandu (conditional composition and uncertainty quantification) Python package developed at the University of Auckland (Dekkers et al., 2022), refined the dataset by filtering models based on how closely the selected blocks beneath the clay cap matched the target temperature of 190°C. Finally, 100 of the most geologically reasonable realizations were selected for further analysis, ensuring an accurate representation of the reservoir's thermal characteristics.

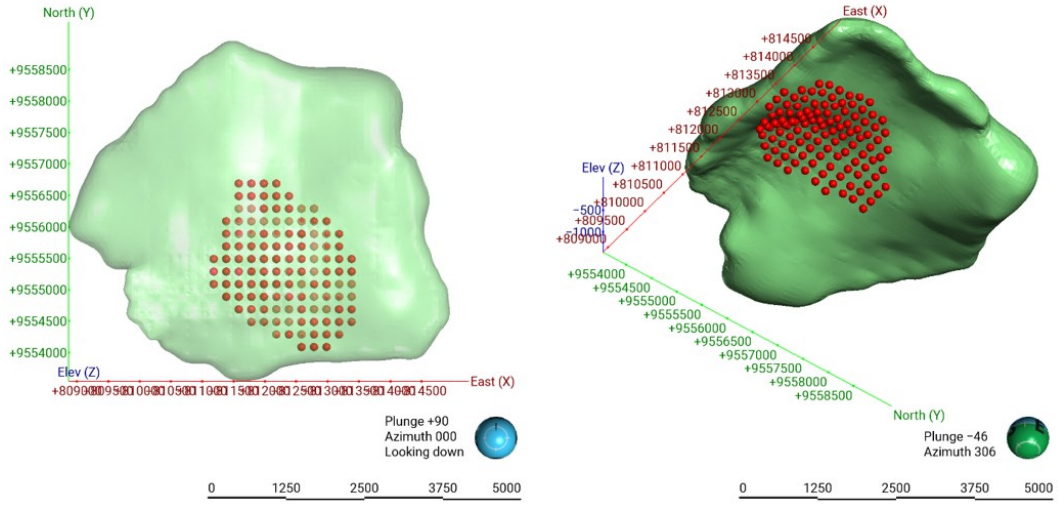


**Figure 10: A top-down perspective (left) and an upward-angled view (right) showing the distribution of block samples used to condition the models positioned directly below the clay cap.**

Figure 10 presents the distribution of blocks beneath the clay cap selected for conditioning. A total of 120 blocks were identified to represent the critical alteration zone, ensuring alignment with the targeted temperature of 190°C. Figure 11 compares the temperature distributions before and after filtering, highlighting how the selected blocks improve model accuracy in replicating observed subsurface conditions.

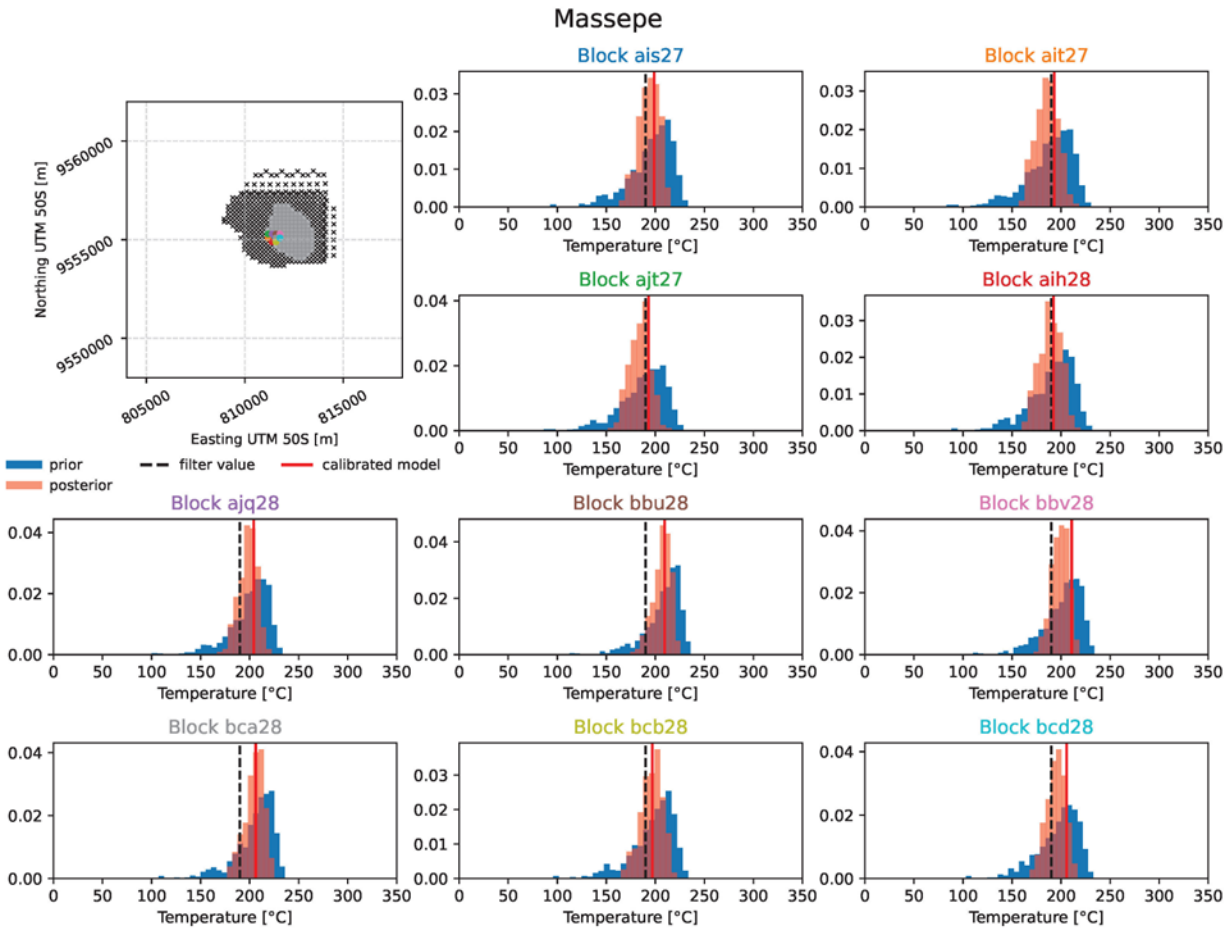


**Figure 11: Comparison of temperature distribution in 10 selected blocks positioned directly under the clay cap: unfiltered (blue) vs. filtered (red).**

Models that meet the temperature criteria are retained for further production simulations, while those that fail to reach the required threshold are excluded. Figure 12 compares the optimal and least favorable sample models, demonstrating variations in temperature distributions beneath the clay cap. The optimal model (#498) successfully reproduces the target temperature of 190°C, reflecting geological constraints within the alteration zone. Conversely, the least favorable model (#104) exhibits significantly lower temperatures, failing to meet the expected conditions.

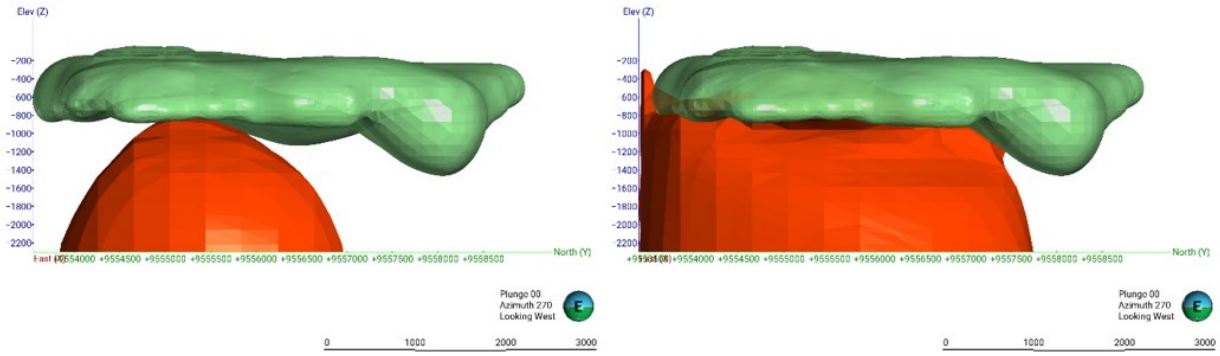

**Figure 12: Comparison of the least favorable samples (left) and the optimal samples (right). The green section represents the clay cap, while the red layer illustrates the temperature distribution at 190°C.**

To better analyze vertical temperature trends, five virtual wells were created in non-residential areas, specifically within rice fields, as determined using Google Maps (Figure 13). These virtual wells can provide a basis for estimating downhole temperatures in future exploration drilling. Figure 14 presents the temperature profiles from these wells, illustrating subsurface thermal gradients and validating the accuracy of the conditioned models.

This whole selection process ensured a robust representation of the geothermal reservoir, balancing accuracy with computational efficiency. The conditioned models were then utilized for further scenario simulations, enabling reliable predictions of geothermal system performance under varying production and reinjection conditions.


**Figure 13: The five virtual wells and three Pajalele hot springs are situated within the Massepe Geothermal Field, as shown on Google Maps.**

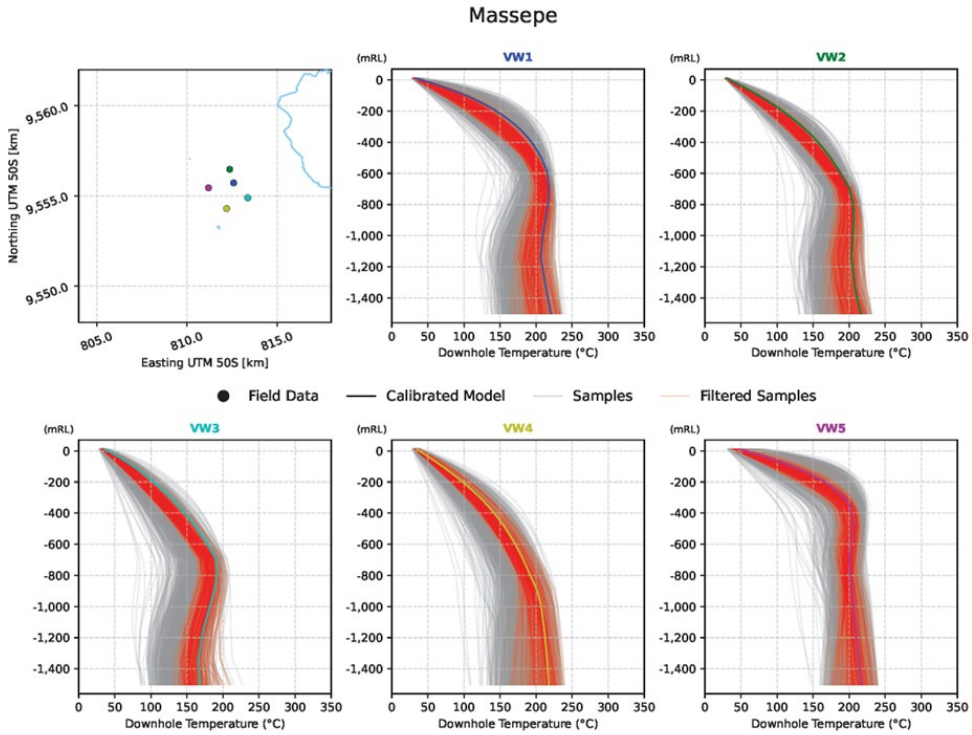


**Figure 14: Downhole temperature profile for five simulated wells in the Massepe Geothermal Field.**

### 5.3 Production Scenario

From the accepted samples, production scenarios were simulated to predict power output and optimize geothermal resource utilization using a binary power plant. The integration of multiple model predictions enabled the estimation of uncertainty ranges, leading to P10, P50, and P90 power output values.

A production forecast algorithm was employed to enhance energy extraction by identifying optimal production and reinjection well placements. These were selected based on flow rates and enthalpy distributions, incorporating pressure-temperature relationships, vapor saturation, productivity index, and wellbore dynamics (Dekkers et al., 2022). The iterative process refined the well configurations until further steam flow rate improvements became negligible.

The maximum drilling depth was set at 1700 meters, with reinjection rates maintained between 70% and 90% of total production to sustain reservoir pressure. A reinjection temperature of 80°C was used as an output from the binary power plant. The algorithm also ensured reinjection wells maintained hydrostatic pressure equilibrium while preventing an excess ratio of reinjection to production wells, which could adversely impact thermal recovery and long-term system stability.

### 5.4 Power Output Forecast

Figure 15 illustrates the projected power output distribution over a 25-year production period. The numerical simulation process involved modeling various production and reinjection scenarios to understand how the geothermal system would behave over time. The model considered different geological and operational uncertainties, including permeability variations, reinjection efficiencies, and well placements.

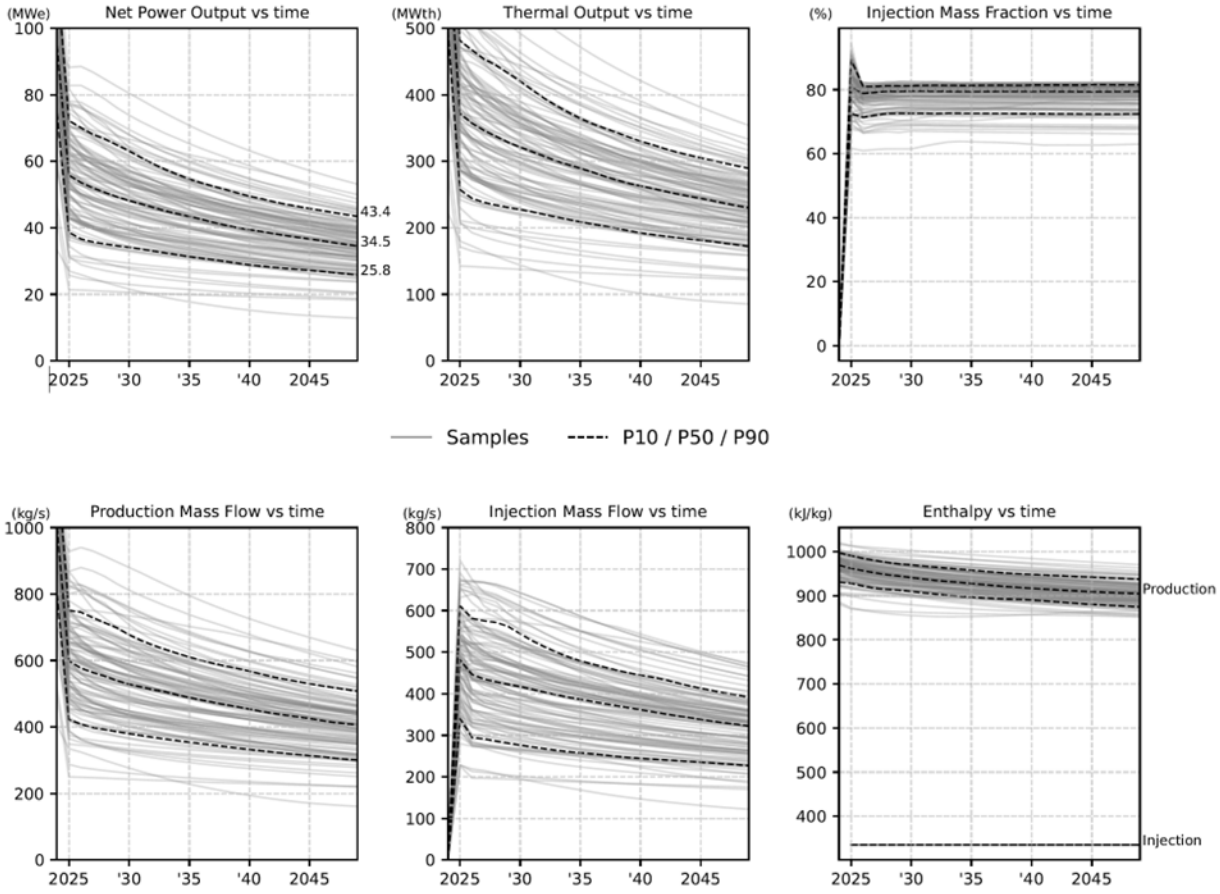


**Figure 15: The total resource potential of the Massepe Geothermal Field. The charts display the estimated range for net power output, thermal output, injection mass fraction, production mass flow, injection mass flow, and enthalpy over 25 years of production, arranged from left to right, top to bottom. The black dashed lines represent the P10, P50, and P90 values derived from sample models, while the grey lines indicate the full range of sample results.**

The results indicate that under conservative conditions, the expected power output is 25.8 MWe, corresponding to the P90 estimate, meaning there is a 90% probability that the output will exceed this value. The P50 estimate, or the most likely scenario, suggests an output of 34.5 MWe, while the P10 estimate, representing the most favorable conditions, projects a maximum potential output of 43.4 MWe.

A combination of small field size and relatively low injection temperature accelerates cold influx within the reservoir, leading to a gradual decline in production enthalpy. This cooling effect negatively impacts production well performance and reduces the total mass available for reinjection, thereby influencing overall reservoir sustainability.

The figure further illustrates power output variations over time, demonstrating how reservoir depletion and pressure drawdown contribute to declining output. However, strategic reinjection plays a crucial role in mitigating these declines by maintaining reservoir pressure and enhancing thermal recovery. The sensitivity analysis performed in the study reveals the importance of permeability distribution and reservoir connectivity in sustaining production rates. The reinjection strategy plays a critical role in stabilizing long-term power output by optimizing thermal recharge and minimizing cooling effects.

## 6. CONCLUSION

This study provides a refined resource assessment of the Massepe Geothermal Field by integrating numerical reservoir modeling with uncertainty quantification. The results indicate a probable power output of 34.5 MWe (P50) over a 25-year production period, with estimates ranging between 25.8 MWe (P90) and 43.4 MWe (P10). The North-South Massepe fault remains the primary geothermal upflow pathway, while an inferred fault to the east introduces notable uncertainty in permeability and fluid flow behavior. The study underscores the critical role of structural permeability in reservoir performance, reinforcing the need for further geological investigations and geophysical surveys to refine resource estimates. These findings contribute to the broader understanding of geothermal energy potential in non-volcanic settings and support the strategic development of renewable energy resources in Indonesia.

## ACKNOWLEDGEMENTS

The authors acknowledge the Directorate General of New, Renewable Energy and Energy Conservation (EBTKE) and the Geological Agency of Indonesia for providing data. The authors also thank Seequent for providing a license for the Leapfrog Energy software, which was instrumental in developing the geological models used in this study. Computational resources were provided by the New Zealand eScience Infrastructure (NeSI).

## REFERENCES

Dekkers, K., Gravatt, M., & O'Sullivan, J. (2022). Resource assessment: Estimating the potential of a geothermal reservoir. Stanford Geothermal Workshop Proceedings.

Joni, W., & Wahyuningsih, R. (2019). Pemodelan inversi 2-D dan 3-D menggunakan data magnetotelurik daerah panas bumi Massepe, kabupaten Sidenreng Rappang, provinsi Sulawesi Selatan. Buletin Sumber Daya Geologi, 14(2), 143–155. https://doi.org/10.47599/bsdg.v14i2.248

Popineau, J., O'Sullivan, J., O'Sullivan, M., & Archer, R. (2018). An integrated Leapfrog/TOUGH2 workflow for geothermal production modeling. 7th African Rift Geothermal Conference.

Pruess, K., Oldenburg, C., & Moridis, G. (1999). TOUGH2 user's guide version 2. Lawrence Berkeley National Laboratory. https://tough.lbl.gov/assets/docs/TOUGH2_V2_Users_Guide.pdf

Rahmansyah, F., Gravatt, M., & O'Sullivan, J. (2024). A 3D Geological Model and Natural State Simulation of the Massepe Geothermal Field. IIGCE Proceedings.